Available online at www.sciencedirect.com
SCIENCE DIRECT®
Journal of Catalysis 231 (2005) 468–479
JOURNAL OF CATALYSIS
www.elsevier.com/locate/jcat

Platinum-tungstated zirconia isomerization catalysts Part II. Effect of platinum and tungsten loading on the mechanism of isomerization of *n*-hexane: a kinetic study

T.N. Vu [a], J. van Gestel [a,*], J.P. Gilson [a,b], C. Collet [b], J.P. Dath [b], J.C. Duchet [a]

[a] *Laboratoire Catalyse et Spectrochimie, CNRS – ENSICAEN – Université de Caen, 6, Bd. du Maréchal Juin, F-14050 Caen, France*
[b] *Total, ATOFINA Research S. A., Zone Industrielle C, B-7181 Feluy, Belgium*

Received 4 December 2004; revised 30 January 2005; accepted 2 February 2005

Available online 23 March 2005

Abstract

The effect of platinum (0.1–1.5 wt%) and tungsten (14–34 wt%) concentrations on the catalytic properties of platinum-tungstated zirconia catalysts for *n*-hexane isomerization was investigated at 523 K. The influence of hydrogen over a wide range of pressures (2–45 bar) was studied to elucidate the mechanism. The tungstated zirconia samples were prepared by bringing a silica-modified hydrous zirconia into contact with metatungstate, followed by extrusion with an alumina binder, and finally calcination at 1023 K. At constant tungsten loading, the activity and stability increase with Pt concentration and then stabilize. Reaction orders were about 1 for *n*-hexane and strongly negative (−0.8) for hydrogen. Kinetic modeling agrees with a classical bifunctional metal–acid mechanism. The tungsten content increased the isomerization activity up to the tungsten monolayer; the isomerization activity then decreased. This variation was related to the concentration of Brønsted acid sites created by the polytungstate species. Changes in selectivity for the dibranched isomers were related to the metal-to-acid ratio.

Keywords: Silica-stabilized tungstated zirconia; Platinum; *n*-Hexane isomerization; Kinetics; Bifunctional mechanism; Hydrogen effect

1. Introduction

Tungstated zirconia has recently become a very attractive solid acid catalyst for the skeletal isomerization of linear alkanes. Although tungstated zirconias alone are active for butane or pentane isomerization at low temperature, promotion by platinum and the presence of hydrogen demonstrated an enhanced activity, an improved stability, and a high selectivity for branched isomers for both light and longer alkanes [1–6]. When compared with sulfated zirconia, the tungstate species appeared to be more resistant than the sulfates to the loss of active sites during the catalytic and regeneration cycles. They are therefore more stable and robust catalysts.

The presence of platinum, together with an acid component, raises the question of the mechanism for paraffin isomerization. The classical bifunctional metal–acid pathway, involving the hydro–dehydrogenation function of the metal, may be operative, depending on the thermodynamic limitations of the concentration in olefinic intermediates [7,8]. Recent studies suggest a nonclassical bifunctional mechanism, in which platinum activates hydrogen and the hydrocarbon and creates Brønsted acid sites and carbenium ions [4]. This was inferred from the ability of the tungstate species, which are present at intermediate coverage, to form $W^{5+}OH$ groups under reducing conditions. The redox properties of the WO_x species may also initiate the isomerization reaction by activation of the alkane [2,9]. The presence of platinum would increase the concentration of reduced W^{5+} centers and thus the activity. Moreover, activated hydrogen on platinum is a source of hydrides, which might accelerate the desorption steps of the carbenium intermediates [4].

In fact, results are essentially qualitative, often restricted to a comparison between a platinum-free and a platinum-

* Corresponding author. Fax: +33 02 31 45 28 22.
E-mail address: jacob.vangestel@ensicaen.fr (J. van Gestel).

0021-9517/$ – see front matter
doi:10.1016/j.jcat.2005.02.003

promoted catalyst [1,10–13]. Moreover, the influence of hydrogen pressure, when investigated, was limited to a small pressure range [4,14]. Changes in platinum content did not show a proportionality with activity [15], and results were interpreted qualitatively as a loss of metallic properties by strong interaction of the metal with the tungstated zirconia [3,16] or a loss in metal surface area [2]. Dispersion measurements based on hydrogen chemisorption are disturbed by spillover and did not correlate with the effect of platinum on activity [8,16]. It seems, however, that only a few metal centers are necessary to promote isomerization over tungstated zirconia, whereas substantial amounts favor the formation of light products by hydrogenolysis [15,17].

It appears that the platinum/tungstated zirconia working catalyst is a complex system. The effect of platinum may vary with a number of parameters, such as the catalyst preparation and experimental conditions during the catalytic test. Therefore, we have undertaken a systematic study of catalysts based on a silica-stabilized zirconia, to avoid changes in structure and texture with tungsten content. The characterization of the metal and acid functions with loading has been presented in Part I [18]. Brønsted acidity of moderate strength, specific to the polytungstate species, has been identified and quantified in a series of catalysts containing 14–34 wt% W, from the FTIR signal of adsorbed CO. Moreover, the accessible metallic platinum sites have been titrated in the range of 0.1–1.5 wt% Pt by both CO adsorption and toluene hydrogenation.

We wish to report here an extensive kinetic study of *n*-hexane isomerization, including the influence of hydrogen over a wide range of pressure, carried out on a series of platinum-tungstated zirconia samples. The intention is to deduce the mechanism of the reaction, with the objective of gaining a reliable correlation between the activity and the physicochemical properties of the metal and acid components of the catalyst.

2. Experimental

2.1. Catalysts

The platinum-tungstated zirconia catalysts used for isomerization of *n*-hexane have been described in Part I of this series [18]. Briefly, we prepared the catalysts by bringing a gel of zirconium hydroxide (doped with 3 wt% silica) into contact with a solution of ammonium metatungstate at various concentrations, drying the catalysts, and further extruding them with 20 wt% alumina. The final calcination at 1023 K yielded stabilized tetragonal zirconia containing 14–34 wt% W in the ZrO_2–SiO_2–WO_x mixture. The extrudates (5×1.6 mm) were then loaded with platinum (0.1–1.5 wt%) by impregnation with an aqueous solution of H_2PtCl_6, followed by calcination at 753 K. The series of catalysts were denoted yPt/xW/SiZ-Al, where x and y stand for tungsten and platinum contents, SiZ is the silica-stabilized zirconia, and the extension -Al denotes the extruded form of the catalysts.

2.2. Catalytic test conditions

The isomerization of *n*-hexane was carried out at a total pressure of 50 bar and 523 K in a continuous-flow fixed-bed microreactor, loaded with 0.2–1.5 g of the extrudate catalyst diluted in alumina extrudates. The partial pressure of hydrogen was varied between 2 and 45 bar with helium as a diluant, and the pressure of *n*-hexane was set at 1, 3, and 5 bar (total flow rate 500 ml/min). The product gas mixture was analyzed periodically (one analysis every 30 min) online with a Varian 3400 gas chromatograph equipped with a FID and a Chrompack CP-SIL 5CB WCOT fused silica capillary column. Conversions were kept below 30%. The reaction order with respect to *n*-hexane was close to one, which was used to calculate initial rates to minimize error. Before the catalytic test, the catalyst was activated in situ at 673 K (heating rate 3 K min^{-1}) in a dry airflow for 2 h, cooled down to 523 K under flowing dry He, and reduced at 523 K in a dry hydrogen flow for 1 h. The reactant *n*-hexane (SDS, 99%) was dried over activated 3A zeolite. Hydrogen (Air Liquide, grade I) and helium (Air Liquide, grade U) were further purified from water and oxygen contaminants with 3A zeolite and BTS (Fluka) traps.

3. Results and discussion

3.1. Composition and tungsten density

The composition and surface areas of the tungstated zirconia samples are listed in Table 1. Since our catalysts were shaped as extrudates with 20 wt% alumina, the values are also given on a W/SiZ basis. In tungstated zirconia catalysts with various tungsten concentrations, the important parameter is the coverage of the active phase, expressed as W atoms/nm^2 ZrO_2. This parameter is not directly accessible from the BET surface areas of the extrudates. However, the surface of the zirconia support itself can be determined from the size of the zirconia crystallites calculated from the XRD pattern, as described in the previous paper [18]. It yields the geometrical area, S_{geo}, of the zirconia. The value is as high as 173 m^2/g, because the tetragonal structure of zirconia is stabilized with silica. It is not further influenced by tungsten loading. The geometrical areas reported in Table 1 for the W/SiZ component of the extrudates were calculated by weight correction for the tungsten content. The 14–34 wt% W loading corresponds to coverages ranging from 3.2 to 11.4 W atoms/nm^2 of the zirconia carrier, excluding the alumina binder. The tungsten density exceeds the theoretical monolayer (~ 6 W atoms/nm^2 ZrO_2) for catalysts loaded with more than 22 wt% W. The final addition of platinum did not affect the textural properties of the xW/SiZ-Al extrudates.

Table 1
Composition, surface area and surface density of tungstated zirconia extrudates

Sample	W (wt%/g)	W (wt%/g W/SiZ)	S_{BET} (m^2/g)	S_{geo}[a] (m^2/g W/SiZ)	W density (atom/nm^2 ZrO_2)
SiZ-Al	0	0	195	173	0
14W/SiZ-Al	11.4	14.3	158	141	3.2
16W/SiZ-Al	12.8	16.0	156	136	3.9
22W/SiZ-Al	17.4	21.8	146	125	5.8
27W/SiZ-Al	21.9	27.4	126	111	8.1
34W/SiZ-Al	27.2	34.0	109	98	11.4

[a] Geometrical area calculated from the crystallite size of zirconia.

3.2. Isomerization of *n*-hexane: product distribution

Table 2 shows the product distribution in isomers and cracking products for some selected catalysts showing different conversion levels. It can be seen that the selectivity in cracking products is always very low, whatever the conversion level. The distribution within the cracking products is difficult to measure, because the yield of C1 to C5 hydrocarbons is close to the detection limit. However, in general, propane is the major product, and in some cases we found C2 and C4 products in lower quantities.

3.3. General features and mechanism of the isomerization of *n*-hexane: *y*Pt/14W/SiZ-Al catalysts

Without platinum, the activity of the 14W/SiZ-Al tungstated zirconia catalyst for isomerization of *n*-hexane at 523 K was highly selective but very low and was almost stable with time (Table 2). Oxoanion-modified zirconia catalysts are known to deactivate very rapidly due to coking [8]. Therefore, it might be that the deactivation period is achieved before the first analysis. This indirectly confirms that active catalysts in hydroisomerization require Pt. We verified on a tungsten-free sample that platinum supported on zirconia does not catalyze isomerization or hydrogenolysis of *n*-hexane under our experimental conditions. Therefore, the hydroisomerization reaction is governed by the combined action of the two components of the catalyst, tungstate species known to be associated with acidity, and the noble metal.

The characteristics of the reaction, stability, influence of hydrogen pressure, and selectivity, were first examined on the *y*Pt/14W/SiZ-Al catalysts, loaded with 3.2 W atom/nm^2 ZrO_2. We will turn then to the influence of tungsten concentration.

3.3.1. Influence of platinum content on activity and stability

The activity of the *y*Pt/14W/SiZ-Al catalysts containing between 0.1 and 0.8 wt% platinum has been compared at 523 K under 3 bar hexane and 10 bar hydrogen. Fig. 1A shows the variation of the rate constant with time on stream. For all of the samples, two periods can be distinguished. During the first 20 h, the activity steeply decreased and then almost stabilized. It is noteworthy that extrapolation of the activity at zero time gives the same value (within experimental error), independently of the platinum content. Thus, even in the presence of platinum, a fraction of the sites involved in isomerization are poisoned. The two periods can be correctly modeled by a hyperbolic function (Fig. 1B). Accordingly, deactivation during the first hours is less pronounced as the platinum concentration increases, up to 0.5 wt% Pt. Higher loading has no further effect. The stability of the catalyst in the second domain is improved by platinum loading as well. The activity level of the quasi-steady-state catalysts increases with platinum content and reaches a plateau at 0.5 wt% Pt.

This behavior is typical for a classical bifunctional metal–acid mechanism. It is well documented on zeolite-based catalysts. At constant concentration of acid sites, the activity at steady state increases with the number of exposed platinum sites and then levels off [19].

In fact, in the case of zirconia catalysts, the total platinum content is not the right parameter to consider because the accessibility of the metal is strongly dependent on the loading

Table 2
Product distribution and rate constants for some catalysts (10 bar H_2, 500 ml/min, 523 K)

Catalyst	Weight (g)	Conversion (mol%)	Isomerization yield (mol%)				Cracking (mol%)	Rate constant[a]
			22DMB	23DMB	2MP	3MP		
14W/SiZ-Al	0.6	2.29	0.02	0.33	1.11	0.78	0.06	0.9
0.1Pt/14W/SiZ-Al	1.0	8.69	0.10	0.87	4.43	3.26	0.03	2.2
0.5Pt/14W/SiZ-Al	1.0	19.94	0.31	1.11	10.85	7.58	0.09	5.7
22W/SiZ-Al	1.5	14.18	0.28	1.95	6.82	4.67	0.46[b]	2.6
1.0Pt/22W/SiZ-Al	0.25	16.48	0.21	0.95	8.99	6.30	0.03	18.3

[a] Rate constant: mol/(h kg bar).
[b] Essentially C2, C3 and C4.

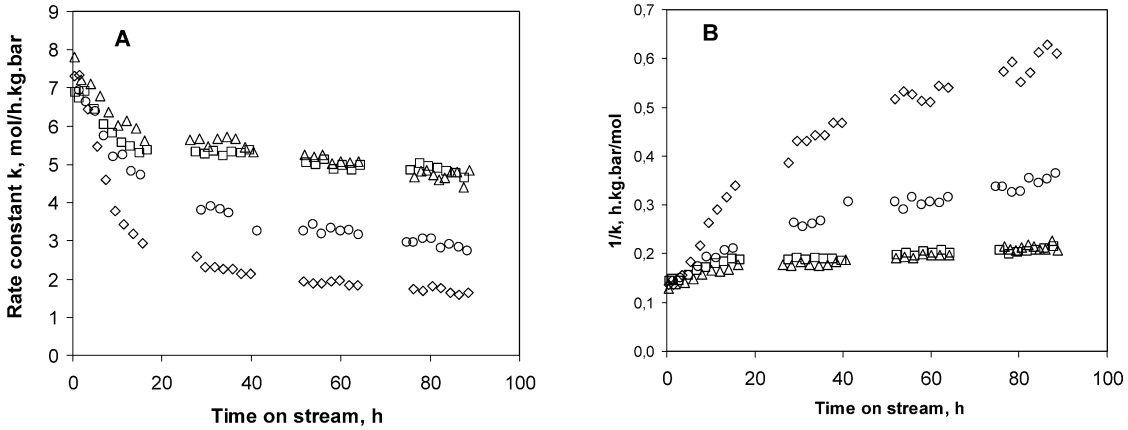

Fig. 1. Isomerization of *n*-hexane over the *y*Pt/14W/SiZ-Al extrudated tungstated zirconia catalysts loaded with 0.1–0.8 wt% platinum. (A) Rate constant versus time-on-stream (523 K, 50 bar total pressure, 10 bar H_2, 3 bar hexane pressure). (B) Hyperbolic transform of the deactivation. (◇) 0.1% Pt; (○) 0.3% Pt; (△) 0.5% Pt; (□) 0.8% Pt.

Table 3
Dispersion of platinum and isomerization activity of the *y*Pt/14W/SiZ-Al catalysts

Sample	Pt loading (wt%)	Pt accessible (μmol/g)	Apparent dispersion[a] (%)	Real dispersion[b] (%)	Particle size (nm)	Isomerization rate constant[c] (mol/(h kg bar))
0.1Pt/14W/SiZ-Al	0.10	1.0	20	67	1.3	2.17
0.3Pt/14W/SiZ-Al	0.30	3.0	20	66	1.3	3.67
0.5Pt/14W/SiZ-Al	0.50	8.3	41	74	1.1	5.67
0.8Pt/14W/SiZ-Al	0.78	22.0	50	70	1.2	5.30

[a] Based on total platinum.
[b] Based on external platinum.
[c] Steady-state activity measured under 10 bar hydrogen.

and other preparation parameters. We have shown that surface platinum concentration is not proportional to the total content because a fraction of the metal is imbedded in the subsurface of the carrier [20]. This phenomenon leads to apparent dispersions well below the dispersion of external Pt. Titration of accessible platinum with CO and hydrogenation of toluene on Pt/W/SiZ-Al catalysts were presented in the previous paper [18]. Values are listed in Table 3 and used to analyze the activity data.

Less than 10 μmol of accessible platinum per gram of catalyst (equivalent to 0.25 wt% external platinum with 70% dispersion) is sufficient to reach the plateau in activity. There is a factor of 2 compared with the total platinum content. This phenomenon does not occur in the case of zeolite catalysts because all of the platinum is accessible.

The amount of accessible platinum is also an important parameter for efficient regeneration of the catalysts. After the first 80 h on stream, the samples were reactivated in situ with air at 673 K. Under these conditions the treatment does not restore the initial activity of the 0.1 wt% Pt catalyst. Rather, the catalyst is quasi-stable right from the start, with an activity level equal to that of the second period of the fresh sample. Most probably the concentration of accessible platinum is too low to eliminate the coke under air at 673 K. By contrast, regeneration of the 0.5 wt% Pt is fully achieved since the catalyst behaves in the second run as a fresh sample, including the deactivation period.

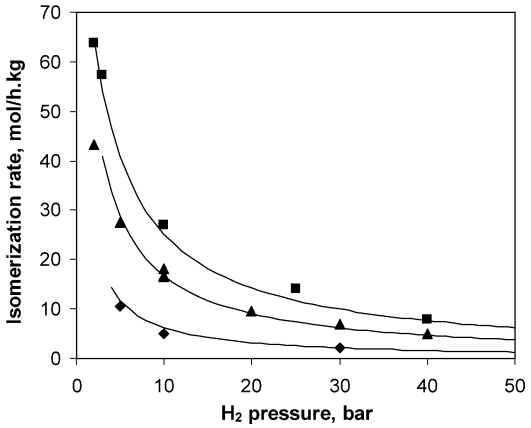

Fig. 2. Influence of hydrogen and *n*-hexane pressures on the isomerization rate at 523 K over the 0.5Pt/14W/SiZ-Al catalyst. (◆) 1 bar Hx; (▲) 3 bar Hx; (■) 5 bar Hx.

3.3.2. *Influence of hydrogen pressure*

The isomerization rates of 1, 3, and 5 bar *n*-hexane have been measured at hydrogen pressures up to 40 bar on the series of *y*Pt/14W/SiZ-Al catalysts. Fig. 2 shows as an example the influence of hydrogen on the sample containing 0.5 wt% Pt. Reaction rates were measured at steady state. Results obtained at very low hydrogen pressures were not meaningful for kinetics because the catalyst rapidly deac-

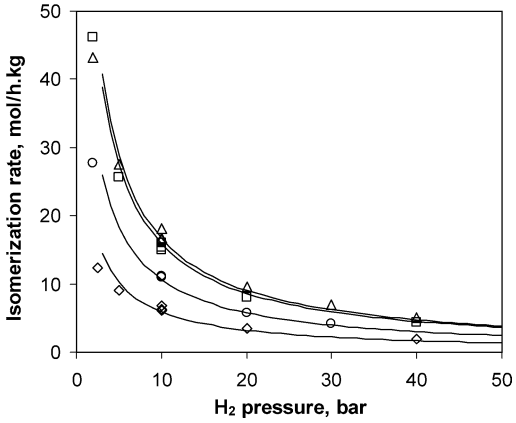

Fig. 3. Influence of hydrogen pressure on the *n*-hexane isomerization rate (3 bar hexane, 523 K) over the *y*Pt/14W/SiZ-Al catalysts at various platinum concentrations. (◇) 0.1% Pt; (○) 0.3% Pt; (△) 0.5% Pt; (□) 0.8% Pt.

tivated. Therefore, only the data obtained under hydrogen pressures higher than 2 bar are plotted on Fig. 2.

Whatever the hexane pressure, hydrogen has a strong negative effect on isomerization with a reaction order equal to −0.8. The reaction is close to first order with respect to the alkane, regardless of hydrogen pressure. These features bear the fingerprint of a classical bifunctional metal–acid mechanism reported on zeolitic catalysts [19,21,22].

The inhibiting effect of hydrogen pressure on isomerization described for the 14W/SiZ-Al sample containing 0.5 wt% Pt is a general phenomenon, observed for all platinum contents. Fig. 3 gathers results obtained at 3 bar hexane on the stabilized catalysts. The positive effect of platinum up to 0.5 wt% on activity, already observed at 10 bar hydrogen (Fig. 1), is again displayed regardless of the hydrogen pressure. This behavior is expected for a classical bifunctional metal–acid mechanism.

3.3.3. Kinetic modeling

The classical bifunctional metal–acid catalysis proposed by Weisz [23] and developed by Coonradt and Garwood [24] offers a good interpretation of the changes in activity and stability with platinum content and the inhibiting effect of hydrogen. These features are encountered with metal-zeolite catalysts [19,21,22]. The reactions taking place in the bifunctional process are recalled in Scheme 1. The metal function generates or hydrogenates the intermediate olefins in steps (1) and (5), and the neighboring acidic function catalyzes isomerization through carbenium ion chemistry.

The skeletal rearrangement of the carbenium ion in step (3) is assumed to be slow, whereas the other steps, especially hydro–dehydrogenation on the metal, are equilibrated. The negative effect of hydrogen is then attributed to a lower concentration in olefinic intermediate. The kinetic treatment of the sequence of elementary steps yields the rate equation,

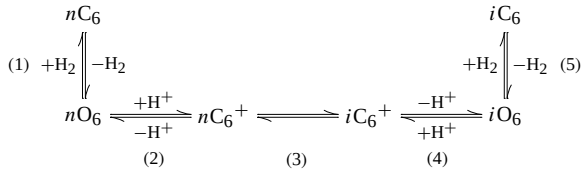

Scheme 1. Elementary steps in the bifunctional isomerization mechanism [19].

which, at initial conversion, is expressed by

$$r^\circ = \frac{k_i B K_1 K_2 P^\circ_{nC_6}}{P_{H_2} + K_1 K_2 P^\circ_{nC_6}} \quad (1)$$

where k_i is the rate constant of the isomerization step (3); K_1 and K_2 are the equilibrium constants, respectively, of the dehydrogenation step (1) and the formation of the carbenium ion in step (2); and B is the concentration of Brønsted acid sites active for isomerization.

This equation, in which the hydrogen term in the denominator accounts for the inhibiting effect, has been reported frequently [22,25]. Only measurements at steady state were considered for the kinetic modeling of the reaction.

Plotting the linear transform $1/r^\circ$ versus the ratio P_{H_2}/P_{nC_6} checked the equation. The straight lines in Fig. 4A verify that the model takes into account the inhibiting effect of hydrogen whatever the hexane pressure. They allow determination of the kinetic parameters, lumped as $k_i B$ and $K_1 K_2$ for various platinum contents. The values were used to draw the curves on Fig. 2 corresponding to the rates measured on the 0.5Pt/14W/SiZ-Al catalyst at 1, 3, and 5 bar hexane. The fit with the experimental data is good. The influence of hydrogen on the other *y*Pt/14W/SiZ-Al samples of the series (Fig. 3) is also adequately modeled by the kinetic equation. The variation of the optimized values of the parameters $k_i B$ and $K_1 K_2$ with the amount of accessible platinum is plotted in Fig. 4B.

The parameter $K_1 K_2$ does not show a significant trend and can be considered approximately constant, as should be expected for the equilibrated steps of the isomerization sequence. From the mean value of the product $K_1 K_2$, around 1.0, and knowing K_1 from thermodynamic tables, it is possible to estimate K_2 to be about 2.5×10^3 bar^{-1}. The equilibrium for the protonation of the olefin is largely in favor of the carbenium ion.

The second parameter $k_i B$ reflects the increase in activity up to ∼ 10 μmol/g accessible platinum (0.5 wt% total Pt) and then tends to stabilize. The observed changes in $k_i B$ must be attributed to the concentration of active acid sites B, since there is no reason for the rate constant of the isomerization step k_i to vary in the series. Indeed, the strength of the Brønsted acid sites is not influenced by platinum [18]. The interpretation for this could be that platinum protects from deactivation the neighboring acid sites within a certain radius, by a spillover process of hydrogen. Increasing platinum loading increases the number of protected/active

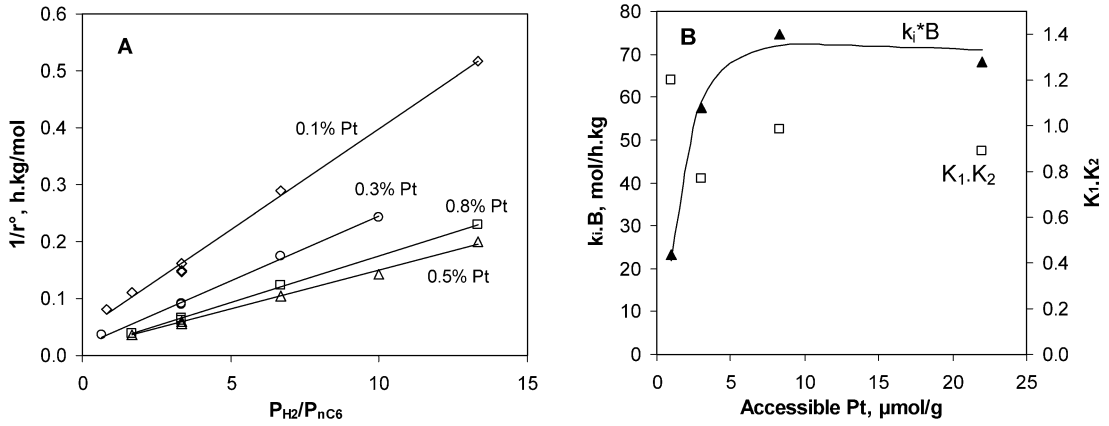

Fig. 4. Check of the kinetic Eq. (1) for the isomerization over the yPt/14W/SiZ-Al catalysts. (A) Linear transform of the initial isomerization rate $r°$. (B) Variation of the kinetic parameters as a function of accessible platinum.

domains and maintains a high activity. The limit at 0.5 wt% platinum corresponds to a geometrical effect, where the protected domains would start to overlap. It should be mentioned that even for catalysts with sufficient accessible platinum ($\gtrsim 10$ µmol/g), a deactivation period is still observed. The changes in selectivity during the deactivation period (see next section) lead us to believe that it corresponds to some poisoning of the metal sites.

3.3.4. Selectivity

According to the bifunctional mechanism, the selectivity among isomers is strongly dependent on the metal-to-acid ratio, that is, the relative number of metal and acid sites, $n\text{Pt}/n\text{A}$. In the case of our yPt/14W/SiZ-Al series of catalysts, only the metal function has been varied, at constant acidity, and we have quantified the amount of accessible platinum. The changes in selectivity will allow us to specify the reaction scheme.

Whatever the platinum content of the yPt/14W/SiZ-Al catalysts, the monobranched isomers 2-methylpentane (2MP) and 3-methylpentane (3MP) were found in their thermodynamic ratio. The changes in selectivity brought about by platinum concern the formation of 2,3-dimethylbutane (23DMB) and 2,2-dimethylbutane (22DMB) isomers. The plot of isomer yield versus conversion obtained at various contact times and hydrogen pressures is shown in Fig. 5 for the series of catalysts at the steady state. The selectivity is given by the yield-to-conversion ratio. We verified that for a given catalyst, the selectivity was not influenced by hydrogen pressure. Cracking is negligible, as is ring closure.

The highest selectivity in 23DMB is observed on the 0.1 wt% Pt sample with a yield close to the thermodynamic ratio with the monobranched isomers. It results from an apparent primary formation of 23DMB, due to an excess of acidic sites relative to the metal sites. This is also the case for the platinum-free 14W/SiZ-Al sample. The 22DMB isomer is always a secondary product. On this catalyst, isomerization occurs as follows:

$$n\text{C}_6 \rightleftharpoons (\text{MP} \leftrightarrow 23\text{DMB})_{\text{eq}} \rightleftharpoons 22\text{DMB}.$$

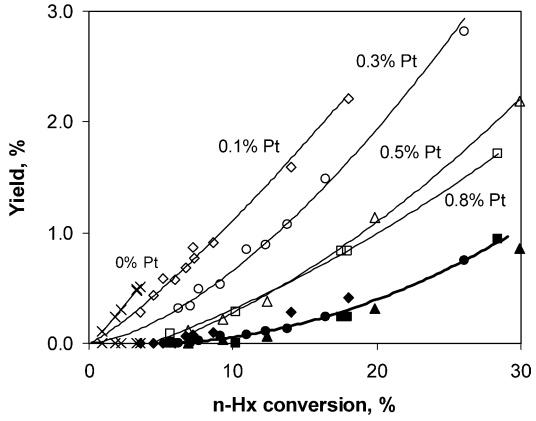

Fig. 5. Selectivity diagram for 23DMB and 22DMB isomers over the yPt/14W/SiZ-Al catalysts (523 K, 2–45 bar hydrogen). Open symbols, 23DMB; filled symbols, 22DMB.

Higher platinum concentrations on the yPt/14W/SiZ-Al catalysts yield 23DMB as a secondary product. The 22DMB isomer remains secondary, but the selectivity diagram cannot indicate a marked effect of platinum. The catalysts containing more than 0.3 wt% Pt illustrate an ideal bifunctional mechanism in which isomerization proceeds through a three-step consecutive reversible reaction scheme:

$$n\text{C}_6 \underset{k_{-1}}{\overset{k_1}{\rightleftharpoons}} (\text{MP})_{\text{eq}} \underset{k_{-2}}{\overset{k_2}{\rightleftharpoons}} 23\text{DMB} \underset{k_{-3}}{\overset{k_3}{\rightleftharpoons}} 22\text{DMB}.$$

Changes in selectivity are also observed during the deactivation period of every catalyst. The 0.1Pt/14W/SiZ-Al catalyst undergoes the largest variations. Considering the yield in 23DMB, its formation corresponds to a nearly ideal behavior at the beginning of the run and progressively turns into an equilibration with the monobranched isomers. As stated in the previous section, this reflects a blockage of some of the platinum sites.

The selectivity in isomers is the result of the relative rates of the three steps of the consecutive reaction scheme. Determination of the rate constant k for each step makes it possible to discriminate the samples for the changes in se-

Table 4
Rate constants of the three-step consecutive reaction scheme for isomerization over the yPt/14W/SiZ-Al catalysts (523 K, 2–45 bar hydrogen)

Catalyst	Pt accessible (μmol/g)	k_1	k_2 (mol/(h kg bar))	k_3
0.1Pt/14W/SiZ-Al	1.0	2.2	28.8	4.7
0.3Pt/14W/SiZ-Al	3.0	3.7	10.3	7.5
0.5Pt/14W/SiZ-Al	10.5	5.7	6.0	16.2
0.8Pt/14W/SiZ-Al	20.0	5.3	4.7	20.2

lectivity with platinum content. Monobranched isomers have been lumped because they are found in their thermodynamic ratio. The data have been treated according to first-order kinetics. The conversion gives access to k_1, and the selectivity diagram was used to optimize the ratio k_2/k_1 and k_3/k_1 by a nonlinear regression method. Values corresponding to isomerization measured under 2–45 bar hydrogen are listed in Table 4.

The variation in the constant k_1 reflects the positive effect of platinum on activity, that is, an increase up to 0.5 wt% followed by a stabilization. The action of platinum on the constant k_2 is the opposite, since we observe a severe decrease at low platinum concentration. The high value of k_2 for the 0.1 wt% Pt sample accounts for the apparent primary formation of the 23DMB isomer. The isomerization of the monobranched tertiary 2- and 3-methylpentyl carbenium ions into the dibranched tertiary 2,3-dimethylbutyl carbenium is an easy process. The large excess of acid sites relative to accessible platinum sites (low nPt/nA) on this catalyst allows the carbenium ions to rearrange several times before they reach a metallic site. Increasing the number of metal sites shortens the distance between the monobranched carbenium ions (and its corresponding olefin) and the hydrogenation sites. The residence time of the monobranched intermediates is diminished. Alternatively, hydrides from hydrogen activated on platinum sites may accelerate the desorption of the isocarbenium ions directly as isoalkanes. The contribution of this pathway would be more important on the high-platinum loaded catalysts. Therefore, the formation of 23DMB from MP becomes a consecutive step through the olefin intermediate pathway, resulting in a decrease in the rate constant k_2.

The increase in k_3 indicates that platinum facilitates the formation of 2,2-dimethylbutane. This is in line with the results of Santiesteban et al. [12], who reported an approach to equilibrium of 22DMB when comparing platinum-free and bifunctional Pt/tungstated zirconia catalysts doped with iron. Again, the generation of hydride species in the presence of platinum may help the secondary 2,2-dimethylbutyl cation to desorb, which otherwise would rearrange into the more stable tertiary 2,3-dimethylbutyl cation. Another possible interpretation advanced by these authors is the hydrogenation of the surface olefinic intermediate, which is in equilibrium with its corresponding carbenium cation. A low concentration of local olefins in the presence of platinum has already been proposed in the mechanism of isomerization over the Pt/H-β catalysts [26]. Thus, the hydrogen transfer reactions promoted by platinum decrease the surface residence time of intermediates on acid sites.

3.3.5. *Bifunctional versus monofunctional mechanism*

Our results on the isomerization of n-hexane over platinum-tungstated zirconia catalysts display the features of a classical metal–acid bifunctional mechanism. This was inferred from the inhibiting effect of hydrogen and from the influence of platinum concentration. Increasing the concentration of accessible metallic platinum increases both the stability and the activity and allows isomerization to proceed from a monofunctional mechanism to an ideal bifunctional behavior.

The literature ascribes to platinum the ability to dissociate hydrogen, but rarely points to an activating function of the alkanes. In fact, the role of platinum may change with the operating conditions. Yori et al. [7], for instance, showed that at low temperature, the two catalytic functions of Pt/WZ catalysts operate independently for n-butane transformations: isomerization on the acid sites, and hydrogenolysis on the metal, while the bifunctional route occurs at 523 K. The olefins involved in the bifunctional mechanism are more easily produced for longer chain alkanes such as n-heptane, allowing the bifunctional mechanism to start at lower temperatures. The reaction of n-hexane may be dictated by the same constraints. Indeed, Falco et al. [8] did not find a significant influence of platinum concentration on the conversion at 473 K, 5.15 bar hydrogen, and 0.75 bar hexane. They rejected the bifunctional mechanism because of the very unfavorable thermodynamics of the first step, yielding at most 1.5×10^{-8} bar of olefins. Examination of the internal distribution of isohexanes confirms their conclusion, since it shows a thermodynamic ratio between 2MP, 3MP, and 23DMB, independent of the platinum loading. Under our standard conditions, 523 K, 3 bar hexane, and 10 bar hydrogen, the partial pressure of hexenes amounts to 10^{-4} bar at equilibrium and is no longer unfavorable for a bifunctional mechanism. At 423 K, the olefin partial pressure has decreased by three orders of magnitude. Accordingly, running our catalysts at low temperature should minimize the bifunctional behavior and change the internal selectivity. Separate experiments carried out on the 0.5Pt/22W/SiZ-Al catalyst show that it is effectively the case: starting at 523 K with an almost ideal selectivity, the internal distribution of isomers progressively shifts to thermodynamics with decreasing temperature to 423 K, whereas the activity declines by a factor of about 100. Moreover, in agreement with Yori et al. [7], the deactivation period of the catalyst observed at 523 K bears the sign for a bifunctional behavior. The stability during the first hours on stream is considerably improved with decreasing temperature down to 423 K, as the bifunctional mechanism declines. The lower concentration in olefins minimizes the extent of coking.

The changes in selectivity with platinum concentration deserve attention with respect to the mechanism. The selectivity for catalysts with very low amounts of accessible

platinum is close to the internal equilibrium ratio of 23DMB with 2MP and 3MP. The behavior looks similar to that of a platinum-free sample. In the case of strongly acidic zeolite catalysts, it corresponds to an acid mechanism. This cannot truly apply to tungstated zirconia. Indeed, the moderate acid strength of the tungstated zirconia [18,27] precludes both the protonation of alkanes to form a carbonium ion and the hydride abstraction on a Lewis site. Alternatively, a redox process is often proposed to initiate the carbenium chemistry on WZ isomerization catalysts. The extensive work by the group of Iglesia [1,4,28] demonstrated that in the presence of platinum and hydrogen, the polytungstate species are slightly reduced and accommodate a proton by electron transfer and charge delocalization. The reduced W^{5+} entities also stabilize the adsorbed carbenium ion. Hydrogen atoms may desorb and regenerate the neutral WO_x. Going one step further, the group of Knözinger [2,5,6,9] could identify organic radicals during the alkane reaction over platinum-free samples, acting as precursors of the carbenium ions. Thus, the redox properties of W^{6+} may be an alternative to the strong acid properties for the monofunctional isomerization over the low-platinum WZ catalysts. Therefore, it is not excluded that the changes in selectivity with platinum content are the result of different contributions of the bifunctional and redox mechanisms.

Whatever the process for isomerization, bifunctional or redox, desorption of the reaction intermediates is facilitated in the presence of hydrogen and platinum. Small amounts of platinum are sufficient to ensure a high availability of hydrogen on the surface of the Pt/WZ catalysts [29]. Hydride species produced by hydrogen may help the hydrogen transfer steps, preventing the β-scission and oligomerization of carbocations, and therefore increasing the overall isomerization selectivity over cracking [12]. We have reported previously that on sulfated zirconia, hydrides play a major role in the isomerization mechanism [30] and proposed that they are associated with the fraction of platinum imbedded as cationic species in the subsurface of zirconia [20]. Since such "buried" platinum is also present on tungstated zirconia [18], the generation of hydrides from dissociated hydrogen is likely. Their concentration should increase with hydrogen pressure and enhance the reaction rate. However, the major effect of hydrogen is the inhibition of the first step of the bifunctional scheme.

3.4. Influence of tungsten loading

Similar data on activity, influence of hydrogen, and selectivity were collected for the other yPt/xW/SiZ-Al catalyts. The whole series of tested catalysts covers not only a change in the metal function, but also large variations in the acid function.

3.4.1. Activity

Since the stability and the activity at steady state of the tungstated zirconia catalysts are strongly dependent on the platinum concentration, the effect of tungsten loading on activity should be inferred from samples containing an amount of platinum sufficient to reach the maximum activity. A fair comparison of the Pt/xW/SiZ-Al catalysts can be obtained, however, with the use of the activity values extrapolated at zero time on stream. In this way the platinum concentration is no longer a parameter effecting activity. We determined the rate constants for the Pt/xW/SiZ-Al catalysts at zero time on stream by modeling the deactivation period as described for the yPt/14W/SiZ-Al series. Results obtained at 10 bar hydrogen and 3 bar hexane are plotted as a function of tungsten loading in Fig. 6.

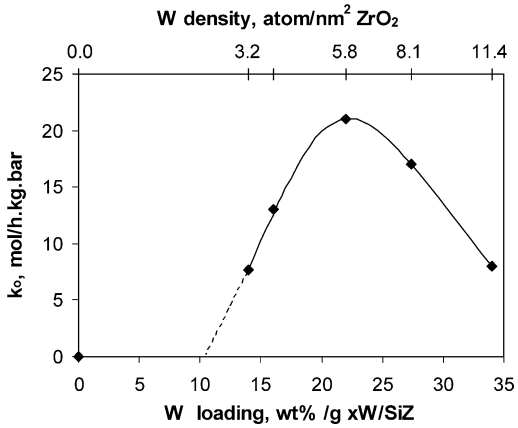

Fig. 6. Isomerization over yPt/xW/SiZ-Al catalysts at 523 K and 10 bar hydrogen. Rate constant at zero time on stream as a function of tungsten loading.

The activity for isomerization reaches a maximum at a concentration of 22 wt% W corresponding to a monolayer coverage of tungsten, that is, ~ 6 W atoms/nm^2 zirconia. Catalysts with a higher W loading show lower activity because of bulk WO_3 formation. The activity in the ascending part of the curve varies almost linearly at intermediate tungsten coverage up to the monolayer. However, extrapolation at very low loading clearly shows a threshold in activity. Although incomplete, our data suggest tungsten species to be inactive below 10 wt% W (~ 2.5 W atoms/nm^2), at approximately half complete coverage.

Similar features on the influence of tungsten loading on activity are derived from the steady-state isomerization rates measured at various hydrogen pressures. All of the yPt/xW/SiZ-Al catalysts are inhibited by hydrogen as encountered on a bifunctional catalyst and obey the rate Eq. (1).

The curves in Fig. 7A illustrate this behavior for various tungstated catalysts with a platinum content sufficient to reach the highest attainable stable activity. The optimized values of the kinetic parameters are plotted in Fig. 7B. As stated above, the variation in $k_i B$ is meaningful, since it reflects, on the working catalyst, the changes in acid site concentration with tungsten loading. The parallel with activity (Fig. 6) is striking: the same position of the maximum for monolayer coverage and the same threshold at about half

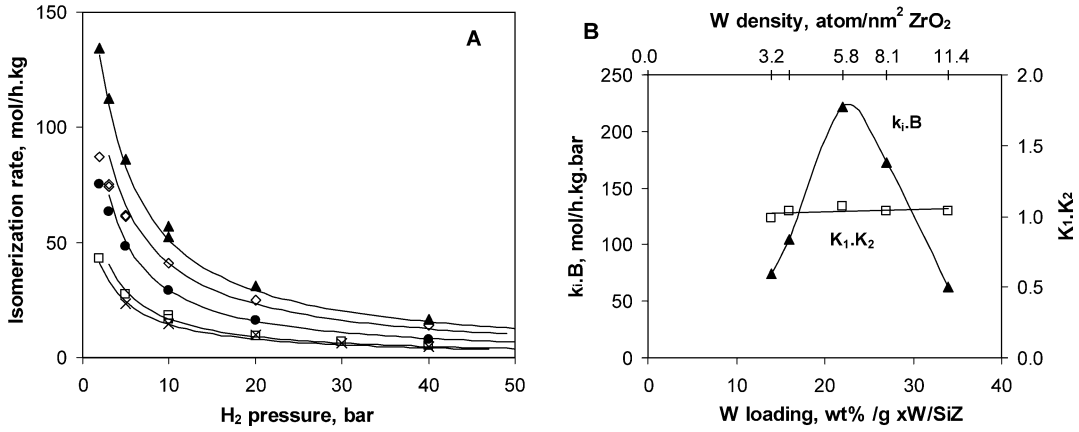

Fig. 7. (A) Influence of hydrogen pressure on the rate for *n*-hexane isomerization (3 bar hexane, 523 K) over the *y*Pt/*x*W/SiZ-Al catalysts at various tungsten concentrations. (□) 0.5Pt/14W/SiZ-Al; (●) 0.5Pt/16W/SiZ-Al; (▲) 1.0Pt/22W/SiZ-Al; (◇) 1.0Pt/27W/SiZ-Al; (×) 1.5Pt/34W/SiZ-Al. (B) Variation of the kinetic parameters of Eq. (1) as a function of tungsten loading.

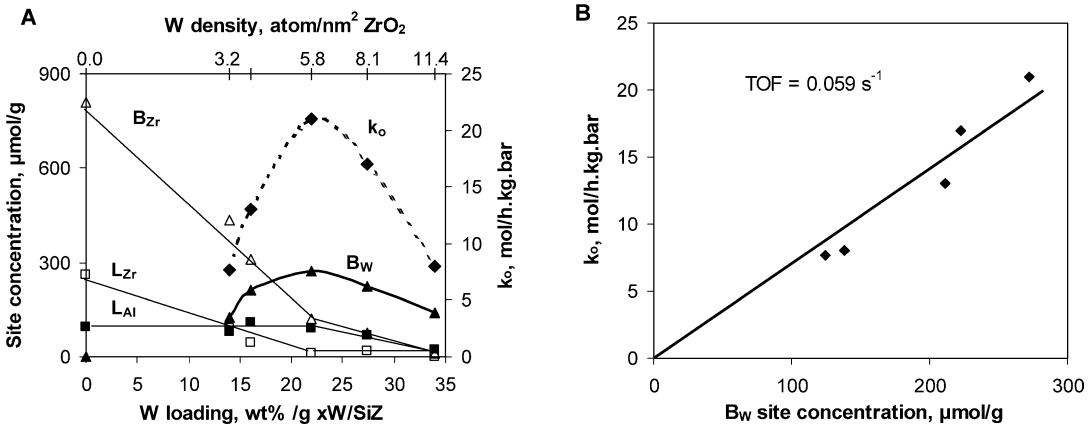

Fig. 8. (A) Variation of the acid site concentration of *x*W/SiZ-Al samples and of the isomerization rate constant at zero time on stream over the Pt/*x*W/SiZ-Al catalysts as a function of tungsten loading. (B) Correlation between the isomerization rate constant at zero time on stream and the concentration of Brønsted acid sites associated with the tungstate phase. See text for the legend.

a monolayer. Thus, provided sufficient accessible platinum is present, the activity is directly related to the acid site concentration. This is discussed in the next section.

3.4.2. Relation between activity and acidity

The acid properties of the series of *x*W/SiZ-Al catalysts have been reported in Part I [18]. The infrared study of carbon monoxide adsorption at low temperature was used to identify and quantify Lewis and Brønsted acid sites. In addition to the Lewis acidity (L_{Al}:$\nu_{CO} = 2191$ cm^{-1}) ascribed to the alumina binder, CO detected the unsaturated Zr^{4+} coordination centers (L_{Zr}:$\nu_{CO} = 2182$ cm^{-1}) of the bare zirconia, not covered by tungsten. Interaction of CO with the Brønsted sites distinguished the weak acidity (B_{Zr}:$\nu_{CO} = 2162$ cm^{-1}) of the zirconia carrier and stronger sites (B_W:$\nu_{CO} = 2167$ cm^{-1}) generated by tungsten. Fig. 8A recalls the variation of the concentration of every type of acidity with tungsten loading. The rate constant k_0 for isomerization at zero time on stream is also plotted in the same figure.

The parallel between activity and the strongest Brønsted acid sites (B_W) is remarkable. Both features appear at intermediate tungsten loading, with a maximum at the monolayer coverage, and yield the correlation of Fig. 8B with a TOF of 0.059 s^{-1}. It demonstrates that on this family of *y*Pt/*x*W/SiZ-Al catalysts, isomerization of *n*-hexane in the presence of hydrogen is controlled by the Brønsted centers associated with tungsten, whereas the Lewis acidity of the solid is unlikely to be involved in the mechanism.

We have discussed in Part I the relation between acidity and the surface structure of the tungstate phase [18]. In brief, the Brønsted acidity associated with tungsten starts to develop at about half the monolayer coverage and increases up to the full W monolayer. At higher coverage, the acid site concentration decreases because of the coexistence of the polytungstates with bulk tungsten oxide. An intermediate tungsten density is therefore critical for the acidity, as well as for the activity.

The quantification of adsorbed carbon monoxide interacting with the Brønsted sites associated with the tungstated zirconia gave a stoichiometry of one H^+ per three W atoms

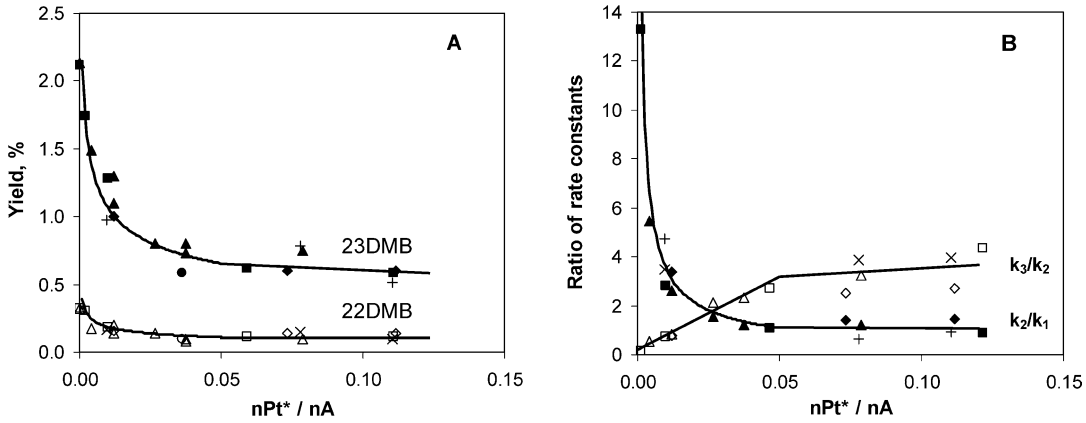

Fig. 9. Selectivity of isomerization over the yPt/xW/SiZ-Al catalysts as a function of the nPt*/nA ratio; the number of accessible metal has been corrected for deactivation. (A) Variation of the yields in 23DMB and 22DMB at 15% n-hexane conversion. (B) Variation of the rate constants ratios for the three steps of the consecutive scheme for isomerization (■, □) 0.5Pt/14W/SiZ-Al; (●, ○) 0.5Pt/16W/SiZ-Al; (▲, △) 1.0Pt/22W/SiZ-Al; (◆, ◇) 1.0Pt/27W/SiZ-Al; (+, ×) 1.5Pt/34W/SiZ-Al.

at maximum tungstate coverage. This high value supports the proposal of Scheithauer et al. [31] for the formation of a pseudo-heteropolyanion incorporating Zr^{4+} ions. On our silica-stabilized zirconia, Si^{4+} may also be involved in a Keggin-like structure. This was inferred from the broad infrared signal around 1100 cm^{-1} in the structure band region, tentatively attributed to interactions between W atoms and the Si–O–Zr surface structure. Very interestingly, the intensity of the signal is maximum for 22 wt% W, corresponding to the monolayer coverage ($\sim$ 6 W/nm^2 ZrO_2). The parallel with the variation of the activity for isomerization further supports the hypothesis that the Brønsted acidity is brought about by the formation of the heteropolyanion species specific to our preparations. Unfortunately, it was not possible to quantify the broad signal, because of a large variation in absorbance of the bare zirconia in this region.

Our results clearly highlight the catalytic role of the polytungstate species at intermediate tungsten coverage, up to $\sim$ 6 W/nm^2 ZrO_2. They markedly differ from those reported in the literature for other acid-catalyzed reactions. Indeed, the maximum activity is found for various tungsten densities, most often significantly higher than the monolayer: 7–8 W/nm^2 ZrO_2 for butanol dehydration [32], 8.2 W for pentane isomerization [33], or $\sim$ 10 W for xylene isomerization [1]. In fact, these values are obtained on solids for which the tungsten density has been varied with the use of two parameters: calcination temperature and loading. By contrast, on homogeneous series, with constant temperature of calcination, the maximum in activity for pentane [27], for butane [34], or for xylene [1] fairly agrees with the monolayer coverage. The nature of the reaction and the presence of platinum seem less critical than the preparation of the tungstated zirconia.

3.5. *Selectivity of platinum-tungstated zirconia catalysts: metal–acid balance*

In the whole series of yPt/xW/SiZ-Al catalysts, the tungsten loading brings changes in the concentration of the acid sites, and the platinum content affects the activity of the metal. We have quantified both functions [18]. The concentration of strong Brønsted sites (nA), correlated with activity, was determined by the IR signal of adsorbed carbon monoxide at low temperature. Accessible platinum (nPt) was measured from toluene hydrogenation and CO adsorption on the metal. Therefore, we may examine the variations in selectivity with respect to the nPt/nA ratio, as usually done for isomerization over bifunctional catalysts. Since 2MP and 3MP isomers are formed in their thermodynamic ratio, we investigated the variation of the dibranched 23DMB and 22DMB products.

The selectivity values are measured at steady state, and the characterization of acidity and platinum refers to fresh catalysts. To be consistent, we should correct the nPt/nA ratio for deactivation. We mentioned in Section 3.4 changes in selectivity during the deactivation period. They suggested a major deactivation of the metallic function rather than of the acid function. We estimated the number of accessible platinum atoms active at steady state, nPt*, using the ratio of activity at zero time on stream and at steady state. Indeed, correcting only the acid function gave erratic variations in selectivity.

A first comparison of the selectivities is shown on Fig. 9A, where the yields in 23DMB and 22DMB obtained at fixed hexane conversion, 15%, are plotted as a function of the corrected nPt*/nA ratio. For the whole series of catalysts, the yield in 23DMB decreases up to nPt*/nA $\sim$ 0.05 and then stabilizes. The yield in 22DMB follows the same features, although in a less sensitive way. The ideal bifunctional behavior is reached at the same value of the metal-to-acid ratio, independently of the tungsten loading. A unique curve is expected because various tungsten contents change the number of sites, but not their strength.

A more complete approach to the changes in selectivity is given by the variation of the rate constants for the three steps of the consecutive reaction scheme. These were determined as described for the yPt/14W/SiZ-Al samples.

However, since the activity and therefore the absolute values of the constants vary widely over the whole series of catalysts, the changes in selectivity are represented in Fig. 9B by the relative values of the rate constants as a function of the corrected parameter $n\mathrm{Pt}^*/n\mathrm{A}$.

The ratio k_2/k_1 concerns the disappearance over the formation of the monobranched isomers 2MP and 3MP, and k_3/k_2 is relative to 23DMB. The data for all of the catalysts fall on the same curves, and both ratios show a singularity for $n\mathrm{Pt}^*/n\mathrm{A} \sim 0.05$. This particularity was already observed on the yPt/14W/SiZ-Al samples. The high value of k_2/k_1 at very low $n\mathrm{Pt}^*/n\mathrm{A}$ indicates that the transformation of 2MP and 3MP into 23DMB is very fast, because of an excess of acid sites. After a sharp decrease, the stabilization of k_2/k_1 for $n\mathrm{Pt}^*/n\mathrm{A} > 0.05$ corresponds to a sufficient accessible metal concentration to supply all of the acid sites in olefinic intermediates and to ensure the desorption of the carbenium intermediates. The eventual contribution of the redox mechanism to isomerization rapidly declines, and the catalysts fully operate in the bifunctional mechanism mode. The 23DMB intermediate is more reactive as the $n\mathrm{Pt}^*/n\mathrm{A}$ ratio increases, but the increase in k_3/k_2 is not followed by a stabilization. Rather, there is a slight enhancement beyond $n\mathrm{Pt}^*/n\mathrm{A} \sim 0.05$. This behavior confirms that platinum is required to achieve the last step of the consecutive sequence. Whatever the tungsten content, an ideal behavior can be obtained, provided there is a proper balance of one accessible metal for about 20 acid sites. Assuming a stoichiometry of one Brønsted site for three tungsten atoms in the Keggin-like structure, one active platinum atom is required for about 60 tungsten atoms.

3.6. Platinum-tungstated zirconia versus platinum-sulfated zirconia catalysts for isomerization

We have reported previously the influence of platinum loading and hydrogen pressure on the *n*-hexane isomerization reaction over platinum-supported sulfated zirconia (Pt/SZ) catalysts [30]. Therefore, it is interesting to compare them with the present results obtained over tungstated zirconia (Pt/WZ). The comparison of the two catalytic systems for isomerization can be reliable only under the same conditions, because the activity depends on both the hydrogen pressure and platinum content. At 423 K, 3 bar hexane, 10 bar hydrogen, the best Pt/SZ catalyst is two orders of magnitude more active than the 0.5Pt/22W/SiZ-Al sample.

The superiority of the sulfated zirconia over the tungstated zirconia comes from different acid properties and results in a different mechanism. Over SZ catalysts, the sulfate groups enhance the strength of zirconia Lewis sites ($\nu_{\mathrm{CO}} \sim 2204\ \mathrm{cm}^{-1}$). By contrast, the polytungstate species consume the zirconia Lewis sites and generate new moderate Brønsted acid sites ($\nu_{\mathrm{CO}} \sim 2167\ \mathrm{cm}^{-1}$). The acidity of the sulfated zirconia is much stronger than that of tungstated zirconia. Pt/SZ and Pt/WZ clearly appear as two different families of catalysts.

The effect of platinum loading and hydrogen pressure on the *n*-hexane isomerization rates is also widely different. Over platinum-supported sulfated zirconia (Pt/SZ) catalysts, the activity increases with hydrogen pressure up to a maximum and then decreases slightly. Increasing the platinum content shifts the maximum to lower hydrogen pressure but does not affect the absolute value of the maximum activity. Platinum has no further effect beyond 0.15 wt%. These features were kinetically modeled by an acid chain mechanism initiated by hydride abstraction on the Lewis sites, and terminated by desorption of carbenium ions assisted by the hydride. Platinum was identified as metal and as cationic species in the subsurface of zirconia. The former dissociates hydrogen and the latter converts the H atoms into the hydrides required for desorption. The maximum in activity with hydrogen pressure results from a competition with the hydrocarbon. This description of the working Pt/SZ catalyst is completely different from the bifunctional mechanism reported here for Pt/WZ catalysts, where hydrogen acts as an inhibitor, and only external metallic platinum plays a major role.

It appears that the nature and the strength of the acid properties of SZ and WZ govern the mechanism for isomerization. Obviously, the two oxoanions do not induce similar effects. The sulfate groups may act by electron withdrawal on the zirconia, which becomes the active phase. In this respect, sulfated zirconia would have features in common with halogenated alumina catalysts. By contrast, tungstate species bring their own moderate acidity, and zirconia may be considered as a carrier. The difference in surface structure may also account for the two distinct families, since the sulfates are grafted to the zirconia as isolated species, whereas WO_x species easily condense to polytungstates, with the ability to eventually form heteropolyanions.

4. Conclusions

The effect of platinum and tungsten loadings on the catalytic properties of platinum-tungstated zirconia catalysts for *n*-hexane isomerization has been examined at 523 K. The influence of hydrogen pressure over a wide range was also studied. The activity results are related to the characterizations of the acid and metal functions.

For all of the Pt/WZ samples, the activity first decreases with time on stream and then stabilizes. At constant tungsten loading, increasing the platinum concentration does not affect the activity at zero time on stream, but increases the steady-state activity up to an accessible platinum-to-acid site ratio of about 0.05.

Hydrogen has a strong negative effect on isomerization activity with a reaction order equal to -0.8. Kinetic modeling agrees with a classical bifunctional metal–acid mechanism.

The isomerization activity of Pt/WZ catalysts increases with the tungsten content up to a maximum at tungsten

monolayer ($\sim$ 6 atom/nm^2 ZrO_2) and decreases beyond. The initial isomerization activity nicely correlates the concentration of moderate Brønsted sites associated with the polytungstate species.

Whatever the platinum content, the monobranched isomers are formed in their internal equilibrium ratio. The selectivity in dibranched isomers 23DMB and 22DMB decreases to the metal-to-acid ratio of 0.05 and then stabilizes, consistent with a bifunctional behavior. The formation of 22DMB is facilitated by the presence of platinum.

Combining an in-depth characterization of the acidic and metallic functions of carefully prepared catalysts with a detailed kinetic analysis of a model reaction is a powerful strategy for uncovering the rules governing the action of a working catalyst. In addition, the insight gained for this catalytic system opens the door to the rational design of isomerization and other catalysts based on tungstated zirconias loaded with a metal function.

Acknowledgments

T.N.V. thanks Total for financial support. We are grateful to Y.L. Tea (Total), M.C. Basset, and J. Quillard (CNRS–ENSICAEN-Université de Caen) for their help with measurements.

References

[1] D.G. Barton, S.L. Soled, G.D. Meitzner, G.A. Fuentes, E. Iglesia, J. Catal. 181 (1999) 57.
[2] S.V. Filimonova, A.V. Nosov, M. Scheithauer, H. Knözinger, J. Catal. 198 (2001) 89.
[3] J.M. Grau, J.C. Yori, J.M. Parera, Appl. Catal. A 213 (2001) 247.
[4] E. Iglesia, D.G. Barton, S.L. Soled, S. Miseo, J.E. Baumgartner, W.E. Gates, G.A. Fuentes, G.D. Meitzner, Stud. Surf. Sci. Catal. 101 (1996) 533.
[5] S. Kuba, P. Lukinskas, R.K. Grasselli, B.C. Gates, H. Knözinger, J. Catal. 216 (2003) 553.
[6] S. Kuba, P. Lukinskas, R. Ahmad, F.C. Jentoft, R.K. Grasselli, B.C. Gates, H. Knözinger, J. Catal. 219 (2003) 376.
[7] J.C. Yori, C.L. Pieck, J.M. Parera, Stud. Surf. Sci. Catal. 130 (2000) 2441.
[8] M.G. Falco, S.A. Canavese, R.A. Comelli, N.S. Figoli, Appl. Catal. A 201 (2000) 37.
[9] S. Kuba, P.C. Heydorn, R.K. Grasselli, B.C. Gates, M. Che, H. Knözinger, Phys. Chem. Chem. Phys. 3 (2001) 146.
[10] S.R. Vaudagna, S.A. Canavese, R.A. Comelli, N.S. Figoli, Appl. Catal. A 168 (1998) 93.
[11] M.G. Falco, S.A. Canavese, N.S. Figoli, Catal. Commun. 2 (2001) 207.
[12] J.G. Santiesteban, D.C. Calabro, C.D. Chang, J.C. Vartuli, T.J. Fiebig, R.D. Bastian, J. Catal. 202 (2001) 25.
[13] J.G. Santiesteban, D.C. Calabro, W.S. Borghard, C.D. Chang, J.C. Vartuli, Y.P. Tsao, M.A. Natal-Santiago, R.D. Bastian, J. Catal. 183 (1999) 314.
[14] G. Larsen, E. Lotero, S. Raghavan, R.D. Parra, C.A. Querini, Appl. Catal. A 139 (1996) 201.
[15] G. Larsen, L.M. Petkovic, Appl. Catal. A 148 (1996) 155.
[16] J.C. Yori, C.L. Pieck, J.M. Parera, Appl. Catal. A 181 (1999) 5.
[17] L.M. Petkovic, J.R. Bielenberg, G. Larsen, J. Catal. 178 (1998) 533.
[18] T.N. Vu, J. van Gestel, C. Collet, J.P. Dath, J.C. Duchet, J. Catal. 231 (2005) 453–467.
[19] F. Ribeiro, C. Marcilly, M. Guisnet, J. Catal. 78 (1982) 267.
[20] J. van Gestel, T.N. Vu, D. Guillaume, J.P. Gilson, J.C. Duchet, J. Catal. 212 (2002) 173.
[21] H. Exner, E. Nagy, F. Fetting, Prepr. Am. Chem. Soc. Div. Petr. Chem. 36 (4) (1991) 853.
[22] M. Guisnet, V. Fouche, M. Belloum, J.P. Bournonville, C. Travers, Appl. Catal. 71 (1991) 295.
[23] P.B. Weisz, Adv. Catal. 13 (1962) 137.
[24] H.L. Coonradt, W.E. Garwood, Ind. Eng. Chem. Prod. Res. Dev. 3 (1964) 38.
[25] G.F. Froment, Catal. Today 1 (1987) 455.
[26] H.Y. Chu, M.P. Rosynek, J.H. Lunsford, J. Catal. 178 (1998) 352.
[27] M. Scheithauer, T.K. Cheung, R.E. Jentoft, R.K. Grasselli, B.C. Gates, H. Knözinger, J. Catal. 180 (1998) 1.
[28] D.G. Barton, S.L. Soled, E. Iglesia, Top. Catal. 6 (1998) 87.
[29] M.G. Falco, S.A. Canavese, R.A. Comelli, N.S. Figoli, Stud. Surf. Sci. Catal. 130 (2000) 2393.
[30] J.C. Duchet, D. Guillaume, A. Monnier, C. Dujardin, J.P. Gilson, J. van Gestel, G. Szabo, P. Nascimento, J. Catal. 198 (2001) 328.
[31] M. Scheithauer, R.K. Grasselli, H. Knözinger, Langmuir 14 (1998) 3019.
[32] C.D. Baertsch, K.T. Komala, Y.H. Chua, E. Iglesia, J. Catal. 205 (2002) 44.
[33] J.G. Santiesteban, J.C. Vartuli, S. Han, R.D. Bastian, C.D. Chang, J. Catal. 168 (1997) 431.
[34] N. Naito, N. Katada, M. Niwa, J. Phys. Chem. B 103 (1999) 7206.